Electronic Supplementary Information

The Enhancement of Photocatalytic Hydrogen Evolution in Imine-Linked Pyrene-based Covalent Organic Frameworks through the Regulation of Active Sites Distance

Jiawen Zong,[a] Huanyu Liu,[a] Wei Lian,[a] Lu Dai,*[a] and Pengfei Li * [a,b]

a Frontiers Science Center for High Energy Material, Key Laboratory of Cluster Science Ministry of Education, Beijing Key Laboratory of Photoelectronic/Electrophotonic Conversion Materials, Advanced Research Institute of Multidisciplinary Science, School of Chemistry and Chemical Engineering, Beijing Institute of Technology, Beijing, 100081, P. R. China

b Advanced Research Institute of Multidisciplinary Science, Beijing Institute of Technology, Zhuhai, No.6, Jinfeng Road, Tangjiawan, Zhuhai, 519088, P. R. China.

*E-mail: luai1104@163.com and lipengfei@bit.edu.cn

Table of Contents

Section S1. Reagents and Instruments

Reagents: All chemicals were commercially available and used without further purification. The 4,4′,4″,4‴-(pyrene-1,3,6,8-tetrayl) tetraaniline (PyTTA) and 4,4′,4″,4‴-(pyrene-1,3,6,8-tetrayl) tetrabenzaldehyde (TFPPy) were purchased from Shanghai Tengqian Biotechnology Co., Ltd and Bide Pharmatech Ltd, respectively. H_2PtCl_6 was purchased from MACKLIN. Ascorbic acid and triethanolamine were purchased from TCI. Glyoxal (40% aqueous solution), 1,4-dioxane, benzyl alcohol, mesitylene, tetrahydrofuran, methanol, and acetone were purchased from Beijing Chemical Regent Company.

Instruments: Fourier transform infrared (FT-IR) spectra were collected in the range of 400-4000 cm^{-1} on Bruker ALPHA spectrometer. Powder X-ray diffraction (PXRD) analysis was carried out on a Rigaku MiniFlex 600 diffractometer operating at 40 kV voltage and 15 mA current with Cu-Kα X-ray radiation (λ = 0.154056 nm). The nitrogen isorption experiment was conducted at 77 K on a Quantachrome Instrument Autosorb-iQ after pretreatment. The specific surface areas were calculated by the Brunauer-Emmett-Teller (BET) method. The pore size distribution was evaluated by the non-local density functional theory (NLDFT). Scanning electron microscopy (SEM) images were acquired from a JEOL model JSM-7500F scanning electron microscope. The samples were sputter-coated with platinum layers to increase their conductivity before observation. UV/Visible diffuse-reflectance (UV/Vis DRS) spectra were collected on a Shimadzu Corporation UV-2600 spectrometer. Photoluminescence and time-resolved PL decay spectra were collected on a Horiba FluoroLog-3 under air. Electron paramagnetic resonance (EPR) spectra were recorded on a JEOL JES-FA200 spectrometer. The contact angles of COFs with water were measured using a drop-shape analysis apparatus (JY-82B Kruss DSA). The zeta potentials were measured with Malvern Zetasizer Nano ZS90. The 300 W Xe lamp with different optical filters were supplied by Microsolar 300, PerfectLight, Beijing. The power density of light used for photocatalysis was tested by THORLABS-PM100D. All electrochemical tests were carried out on CHI 760E electrochemical workstation.

Section S2. Synthetic procedures and measurements

Preparation of Py-COFs

All the Py-COFs are synthesized by using solvothermal methods. A Pyrex tube was charged with 0.04 mmol pyrene-based monomer (TFPPy or PyTTA), 0.08 mmol reactants (amines or aldehydes), and solvents. The resultant mixture was sonicated for 10 min at room temperature and all the reaction systems were added 6 M acetic acid as a catalyst. After three times freeze-thaw operations, the Pyrex tubes were sealed and heated at 120 ℃ for 3 days. The obtained precipitate was washed three times with tetrahydrofuran and acetone and finally dried at 150 ℃ under vacuum.

The composition of solutions is as follows. For Py-COF-1, *o*-dichlorobenzene and n-butyl alcohol in 19:1 with a volume of 2 mL; For Py-COF-2, mesitylene and benzyl alcohol in 1:1 with a volume of 2 mL; For Py-COF-3, *o*-dichlorobenzene and n-butyl alcohol in 1:1 with a volume of 2 mL; For Py-COF-4, mesitylene and 1,4-dioxane in 2:1 with a volume of 3 mL.

Protonation of Py-COFs

Py-COFs (10 mg) were firstly dispersed in 10 mL of 0.1 M ascorbic acid solution. The obtained suspensions were sonicated dispersed for 30 min, and then stirred under N_2 atmosphere for 4 h. Finally, the mixtures were filtered and then activated under vacuum at 60 ºC for 12 h. The protonated COFs were labeled as Py-COF-1 (AC), Py-COF-2 (AC), Py-COF-3 (AC), and Py-COF-4 (AC), respectively.

Photoelectrochemical measurement

To fabricate the working electrode, 5 mg of COF, 1 mL of ethanol, and 10 μL of 5% Nafion in water were mixed under sonication for 30 min to make the sample fully dispersed. The resultant slurry was dropped onto a piece of fluoride-tin oxide (FTO) glass substrate with a cover area of 0.25 cm^2. The uncovered parts of the electrode were coated with epoxy. The working electrode was dried in the air naturally. The photocurrents were recorded by an electrochemical workstation equipped with a conventional three-electrode cell. A platinum plate electrode and an Ag/AgCl electrode were used as the counter electrode and the reference electrode, respectively. The

electrodes were immersed in a 0.2 M aqueous Na_2SO_4 solution (pH = 6.8). The working electrode was illuminated by a 300 W Xe lamp (PLS-SXE300C) with a 420 nm cut-off filter from the backside. Each measurement was repeated three times under ambient conditions.

$$E_{NHE} = E_{(Ag/AgCl)} + E^{\theta}_{(Ag/AgCl)} \ (E^{\theta}_{(Ag/AgCl)} = 0.199 \text{ V})$$

Photocatalytic hydrogen production test

10 mg of COFs was added into 15 mL of 0.1 M ascorbic acid solution, which was sonicated for 30 min to obtain a uniformly dispersed suspension. Then, the 10 μL 40 mg L^{-1} chloroplatinic acid aqueous solution was added to the mixed suspension. The solution was transferred to a photocatalytic sealed reactor and installed in the Labsolar-6A photocatalytic equipment. The 300 W xenon lamp (>420 nm) was used to irradiate the reactor. And the temperature of external cooling circulating water was set at 5 ºC. Before the photocatalytic test, the photo-activation of the reaction solution for 60 min to in-situ form Pt nanoparticles as the co-catalyst. The photocatalytic system automatically takes samples every 30 min and is detected online by gas chromatography.

The experimental condition of the recycle test was identical with the above photocatalytic test. We took 4 hours of continuous photocatalysis as one cycle. The COF catalysts were recovered at the end of each cycle and re-dispersed in 15 mL of 0.1 M ascorbic acid aqueous solution. This process was repeated for three cycles. Finally, the COFs were centrifuged, washed with tetrahydrofuran and acetone, and further characterized.

Determination of apparent quantum yield

The measurement of apparent quantum yield (AQY) for photocatalytic hydrogen production of COFs is similar to the procedure in photocatalytic measurement. The only difference is that under a 300 W Xe lamp with different monochromatic filters (420, 450, 500, 520, and 550 nm). Using an optical power meter (Thorlabs PM100D), the optical power density at each wavelength was 10.2 mW cm^{-2}, and the light emission area was 19.6 cm^2. The AQY was calculated by using the following equation based on the amount of hydrogen produced during the photocatalytic reaction within one hour.

$$\eta_{AQY} = (2 \times M \times N_A \times h \times c) / (S \times P \times t \times \lambda) \times 100\%$$

Where M is the amount of H_2, N_A is the Avogadro constant (6.02×10^{23} mol^{-1}), h is the Planck constant (6.626×10^{-34} J·s), c is the speed of light (3×10^8 m s^{-1}), S is the irradiation area (cm^2), P is the intensity of irradiation light (W cm^{-2}), t is the photoreaction time (s), λ is the wavelength of the monochromatic light (nm).

DFT computational details

All the calculations are performed in the framework of the density functional theory with the projector augmented plane-wave method, as implemented in the Vienna ab initio simulation package.[1,2] The generalized gradient approximation proposed by Perdew-Burke-Ernzerhof (PBE) is selected for the exchange-correlation potential.[3] The cut-off energy for the plane wave is set to 500 eV. The energy criterion is set to 10^{-5} eV in the iterative solution of the Kohn-Sham equation. All the structures are relaxed until the residual forces on the atoms have declined to less than 0.01 eV/Å.

Section S3. Supplementary Figures and Tables

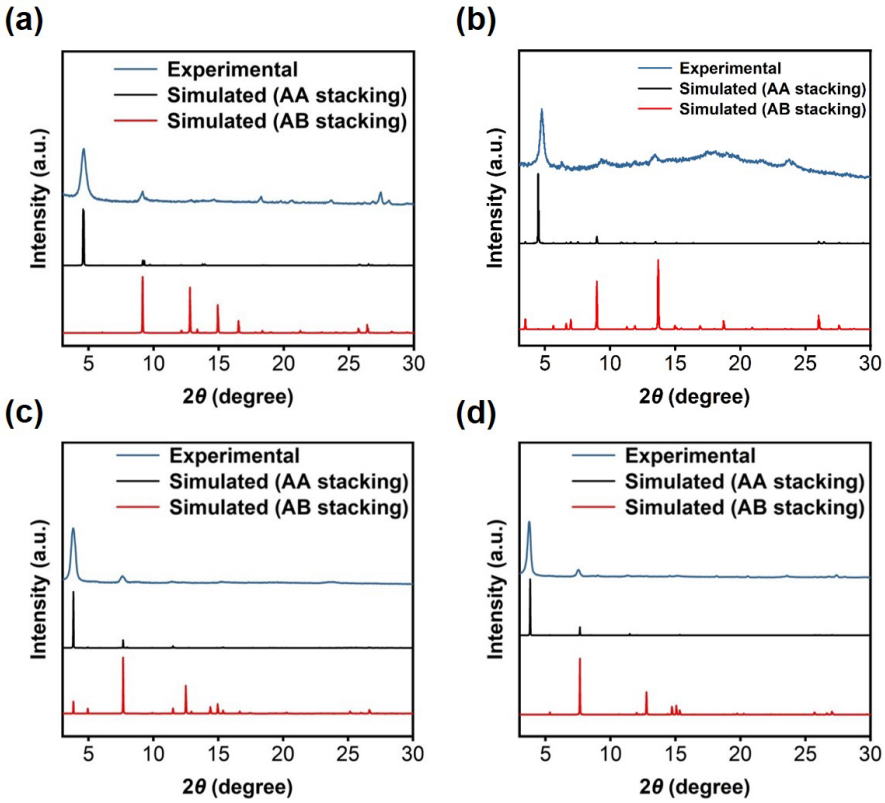

Figure S1. The experimental and simulated PXRD patterns of Py-COF-1 (a), Py-COF-2 (b), Py-COF-3 (c), and Py-COF-4 (d).

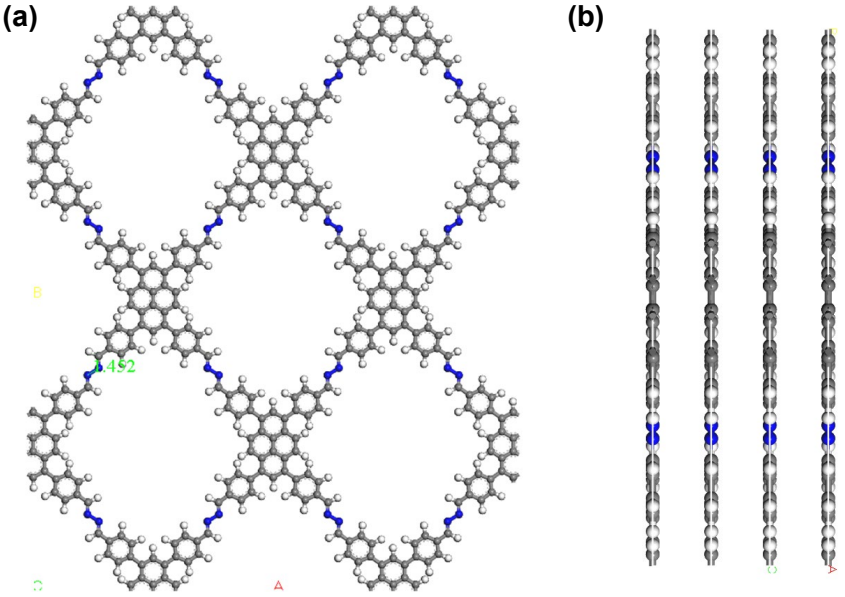

Figure S2. The chemical structure of Py-COF-1 in AA stacking model, (a) top and (b) side view (C, gray; N, blue; and H, white). The green line represents the distance between the N atoms in the diimine bond.

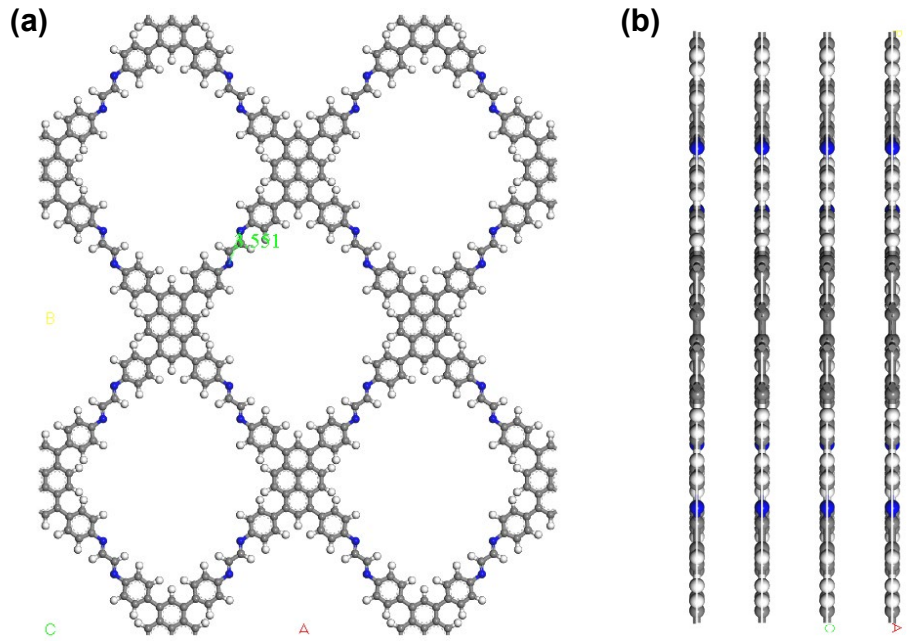

Figure S3. The chemical structure of Py-COF-2 in AA stacking model, (a) top and (b) side view (C, gray; N, blue; and H, white). The green line represents the distance between the N atoms in the diimine bond.

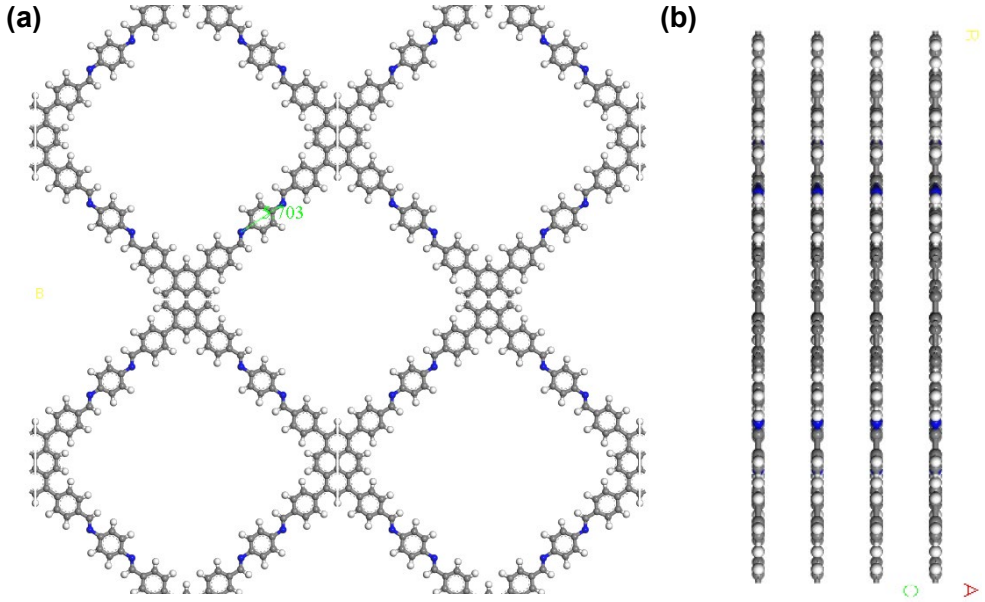

Figure S4. The chemical structure of Py-COF-3 in AA stacking model, (a) top and (b) side view (C, gray; N, blue; and H, white). The green line represents the distance between the N atoms in the imine bond.

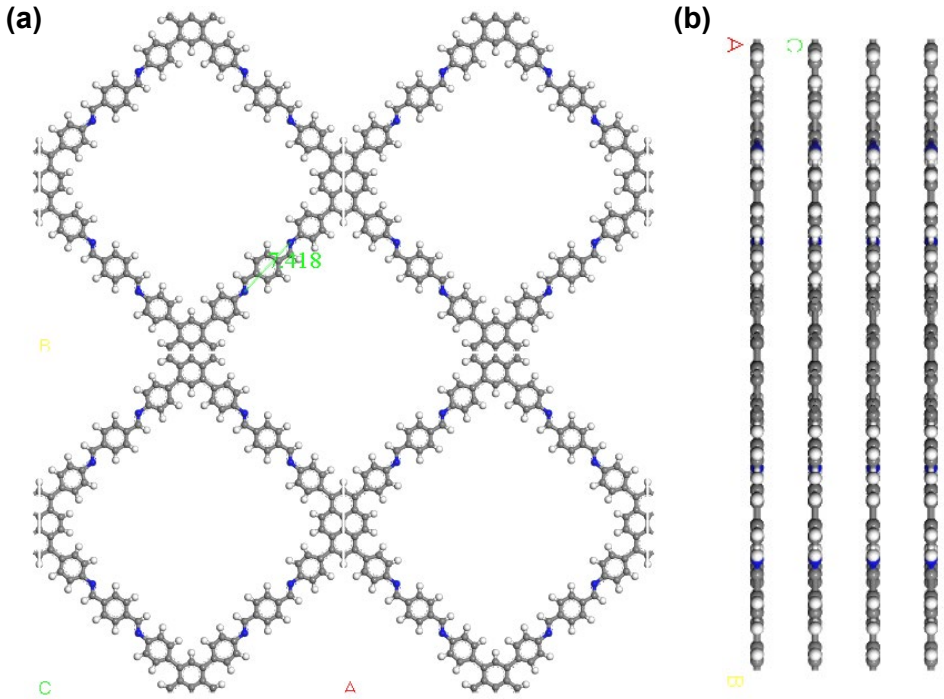

Figure S5. The chemical structure of Py-COF-4 in AA stacking model, (a) top and (b) side view (C, gray; N, blue; and H, white). The green line represents the distance between the N atoms in the imine bond.

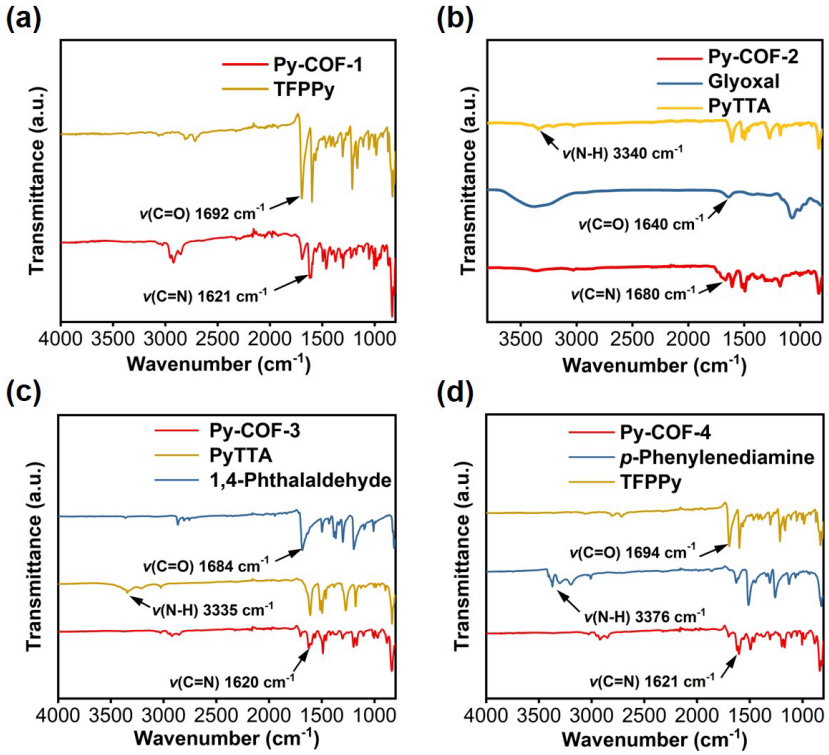

Figure S6. FT-IR spectra for (a) Py-COF-1, (b) Py-COF-2 (c) Py-COF-3 and (d) Py-COF-4.

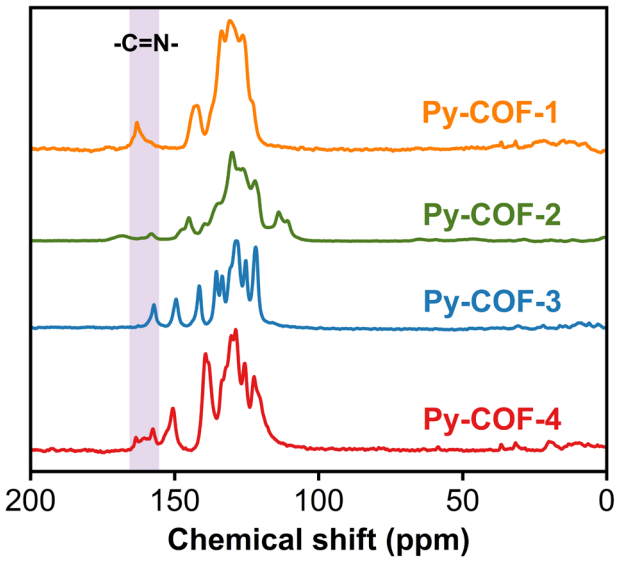

Figure S7. The solid-state ^{13}C CP/MAS NMR spectra of Py-COFs.

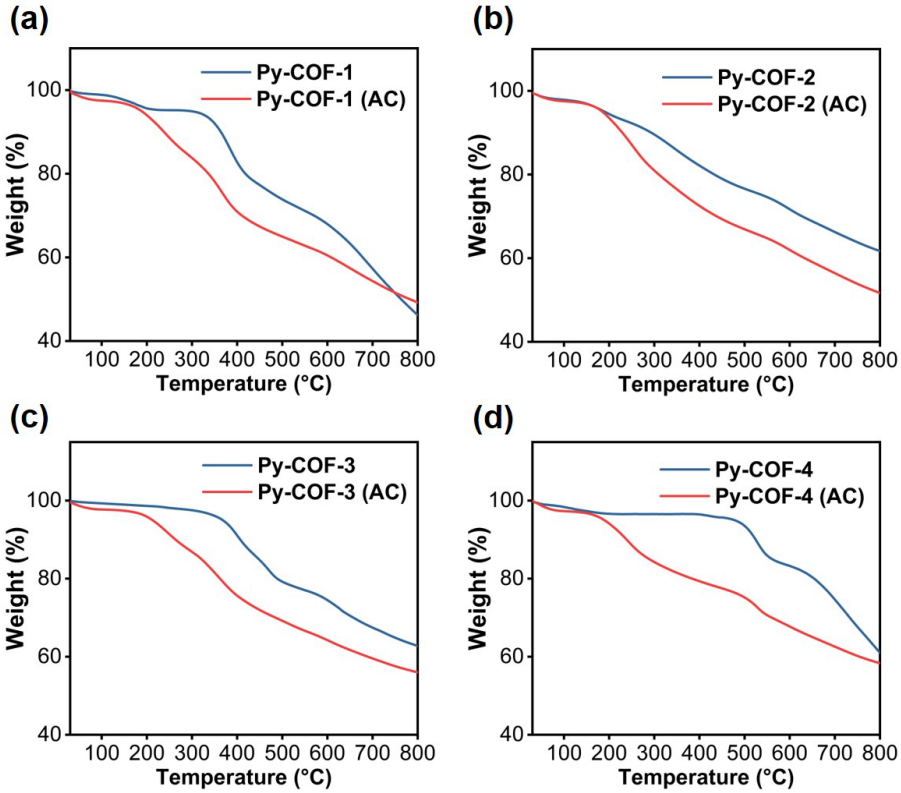

Figure S8. The TGA curves of Py-COFs before and after protonation.

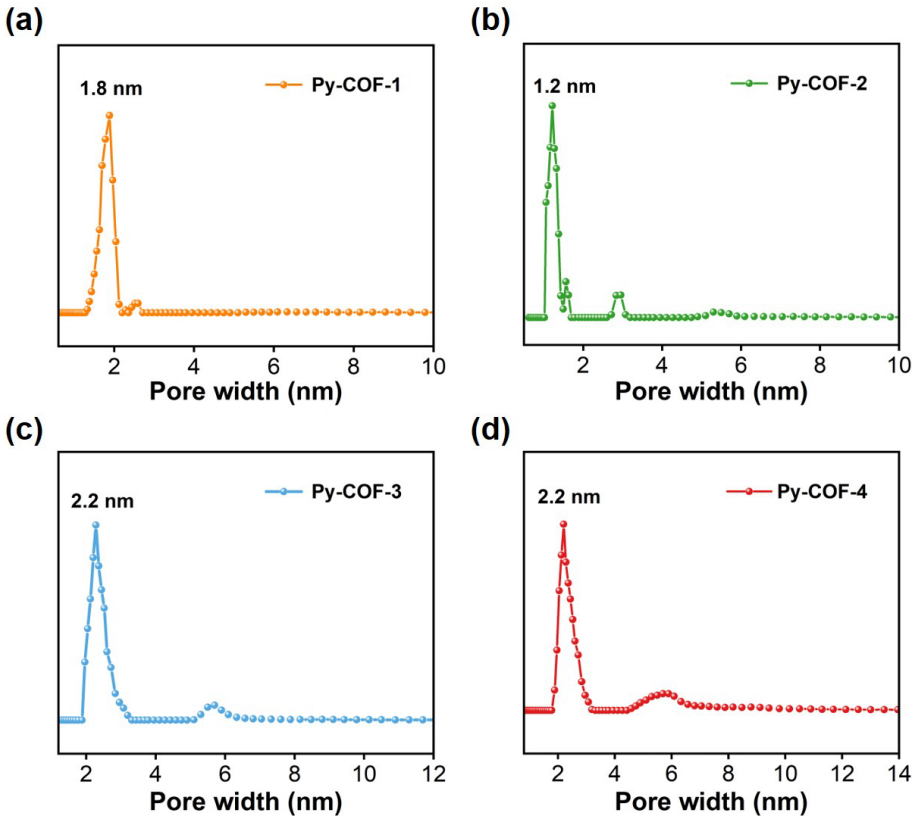

Figure S9. The pore size distributions for (a) Py-COF-1, (b) Py-COF-2 (c) Py-COF-3 and (d) Py-COF-4.

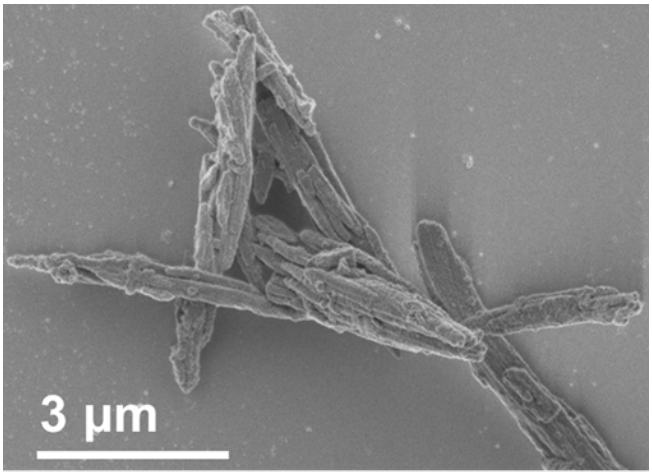

Figure S10. SEM image of Py-COF-1.

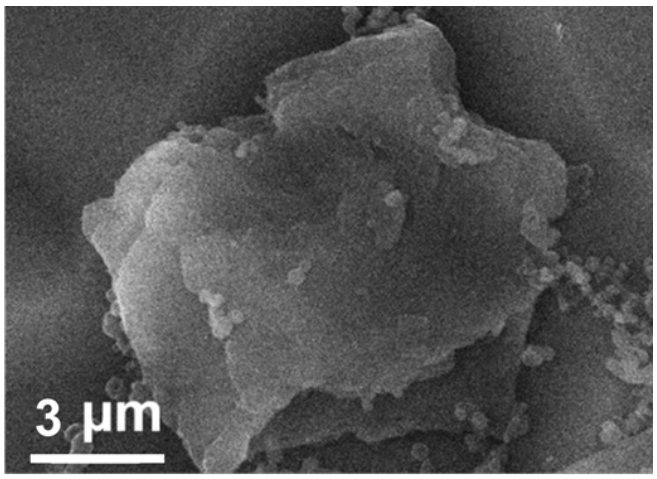

Figure S11. SEM image of Py-COF-2.

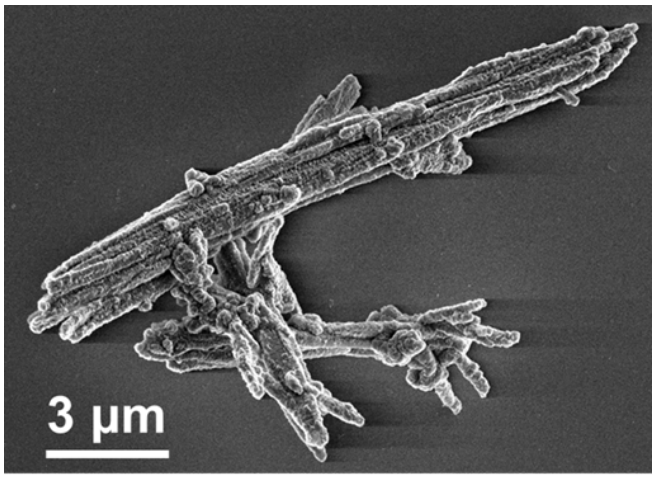

Figure S12. SEM image of Py-COF-3.

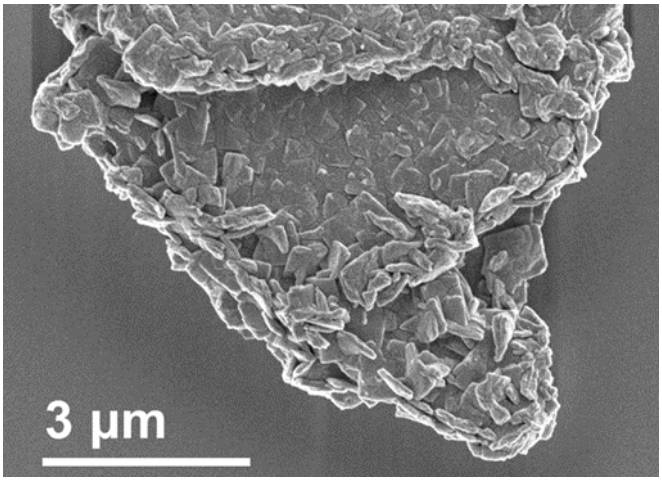

Figure S13. SEM image of Py-COF-4.

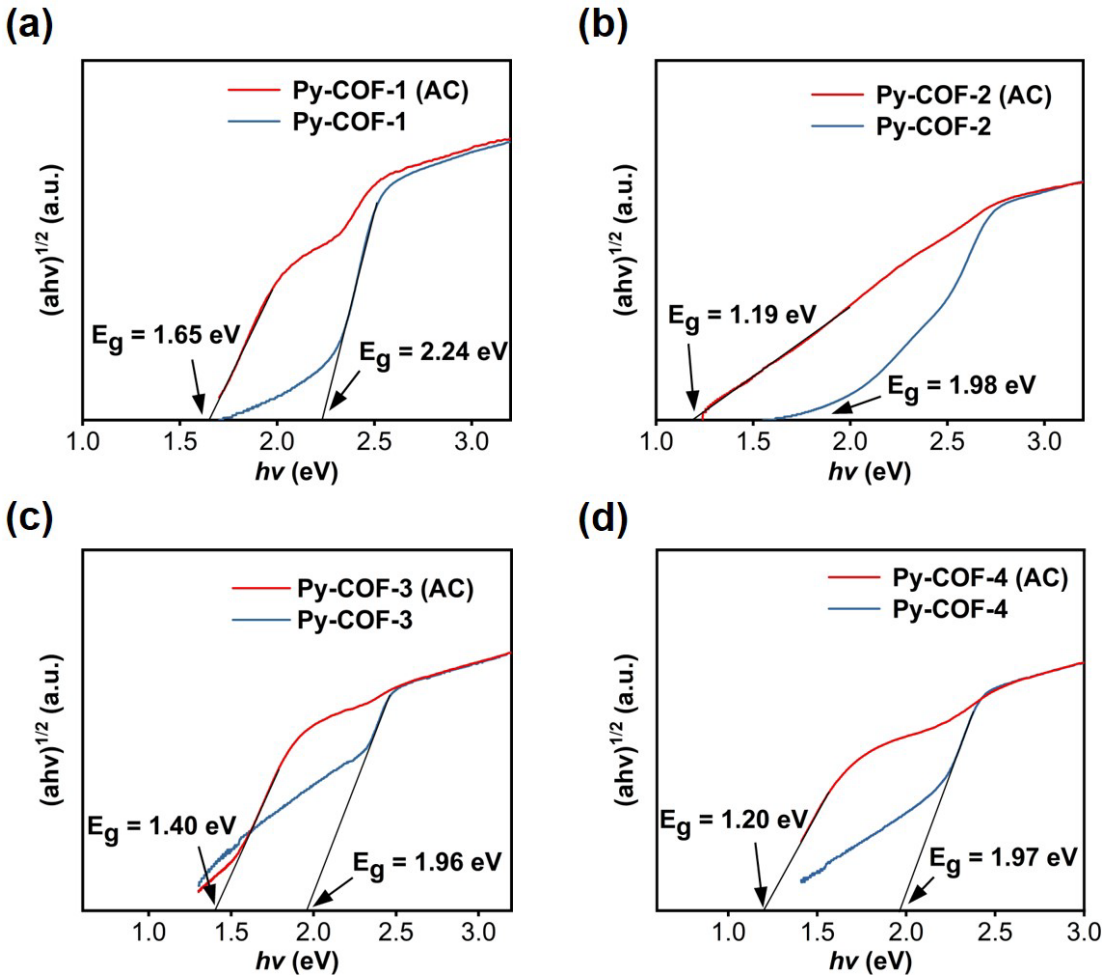

Figure S14. Tauc plots of Py-COFs and Py-COFs (AC).

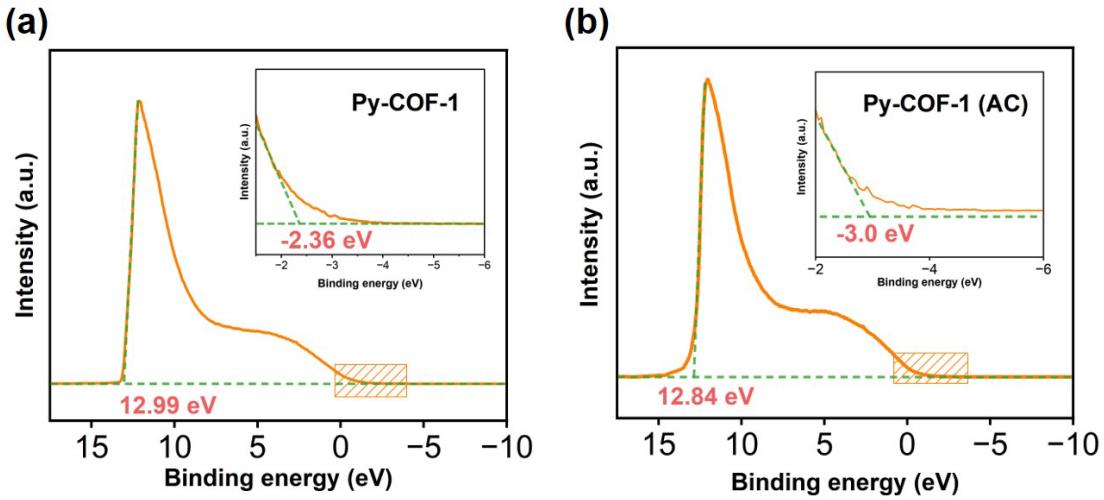

Figure S15. UPS spectra of (a) Py-COF-1 and (b) Py-COF-1 (AC). Note: E_{VB} (vs. NHE) = E_{VB} (vs. vacuum) − 4.44 and E_{VB} (vs. vacuum) = 21.22 + E_{Fermi} − E_{Cutoff}.

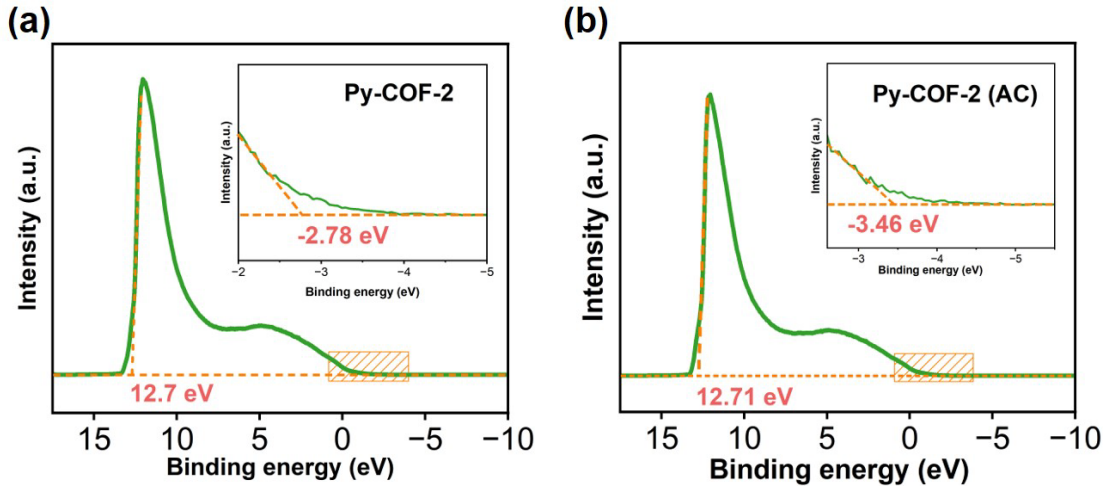

Figure S16. UPS spectra of (a) Py-COF-2 and (b) Py-COF-2 (AC). Note: E_{VB} (vs. NHE) = E_{VB} (vs. vacuum) − 4.44 and E_{VB} (vs. vacuum) = 21.22 + E_{Fermi} − E_{Cutoff}.

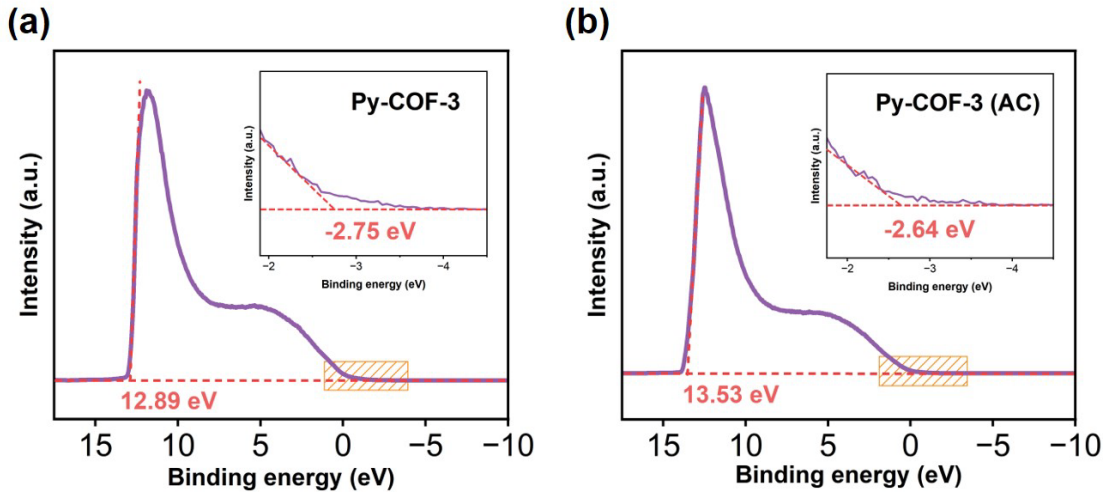

Figure S17. UPS spectra of (a) Py-COF-3 and (b) Py-COF-3 (AC). Note: E_{VB} (vs. NHE) = E_{VB} (vs. vacuum) − 4.44 and E_{VB} (vs. vacuum) = 21.22 + E_{Fermi} − E_{Cutoff}.

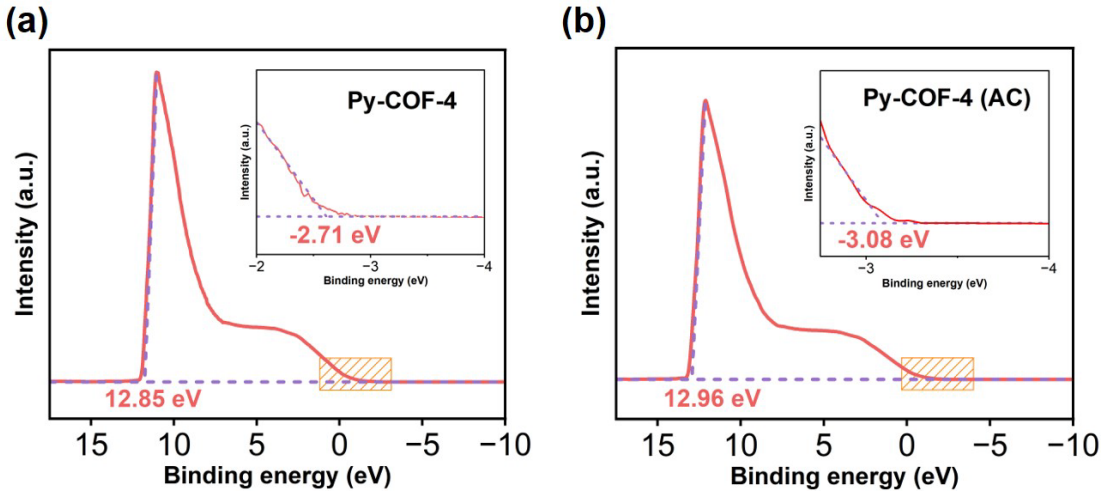

Figure S18. UPS spectra of (a) Py-COF-4 and (b) Py-COF-4 (AC). Note: E_{VB} (vs. NHE) = E_{VB} (vs. vacuum) − 4.44 and E_{VB} (vs. vacuum) = 21.22 + E_{Fermi} − E_{Cutoff}.

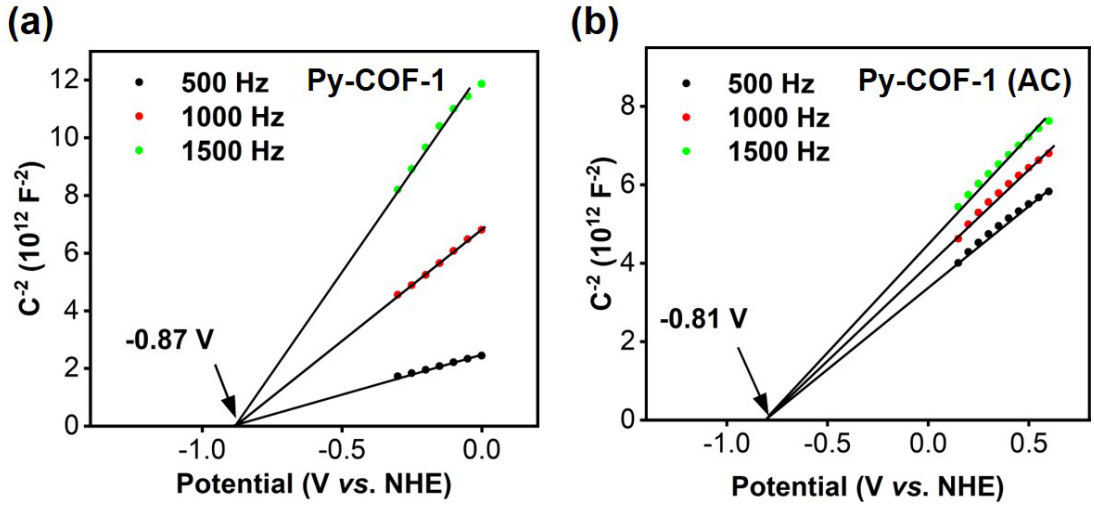

Figure S19. Mott-Schottky plots of (a) Py-COF-1 and (b) Py-COF-1 (AC).

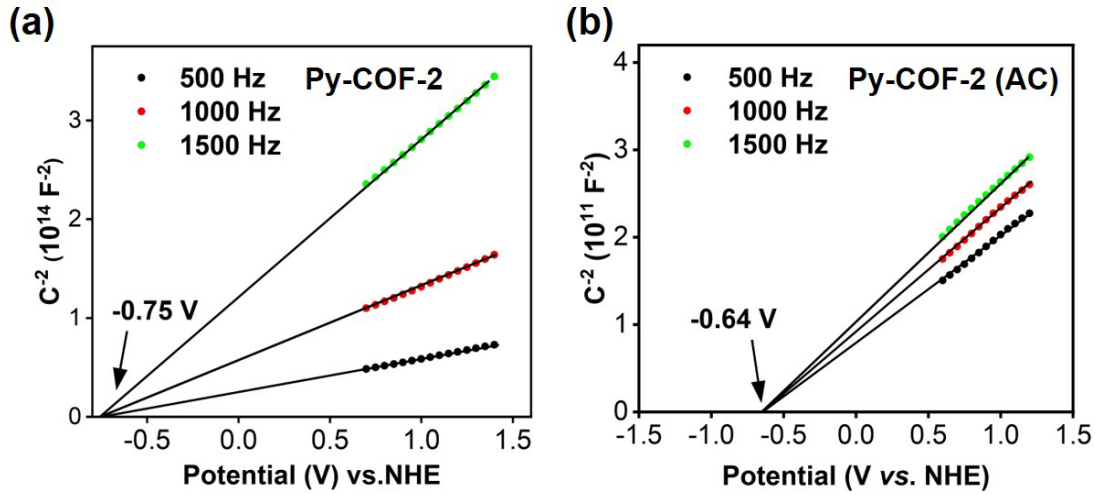

Figure S20. Mott-Schottky plots of (a) Py-COF-2 and (b) Py-COF-2 (AC).

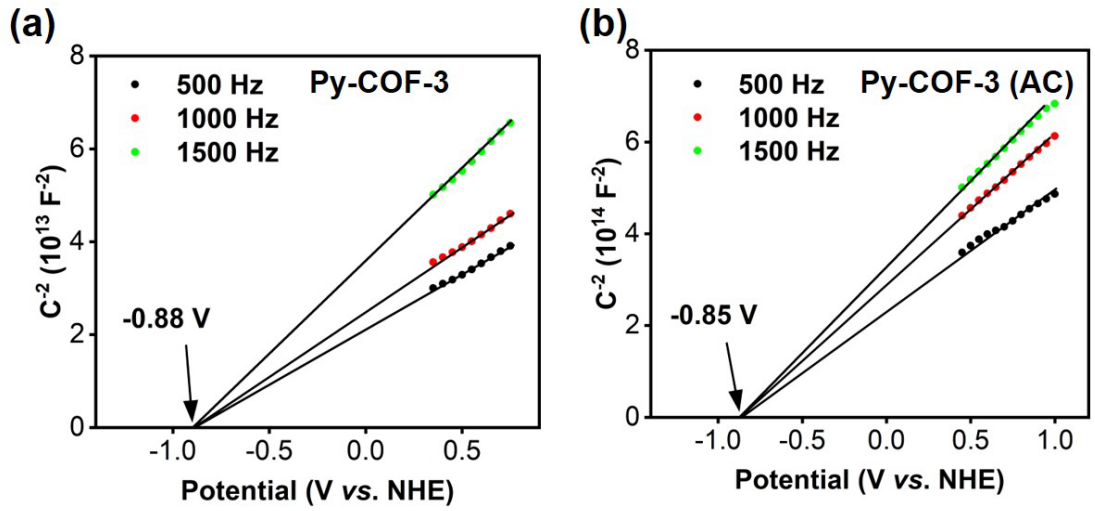

Figure S21. Mott-Schottky plots of (a) Py-COF-3 and (b) Py-COF-3 (AC).

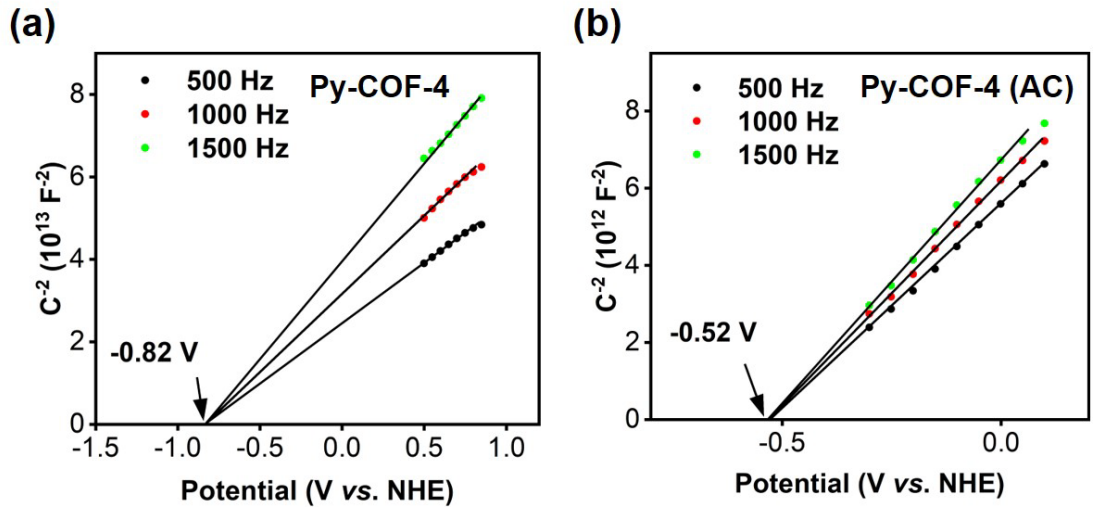

Figure S22. Mott-Schottky plots of (a) Py-COF-4 and (b) Py-COF-4 (AC).

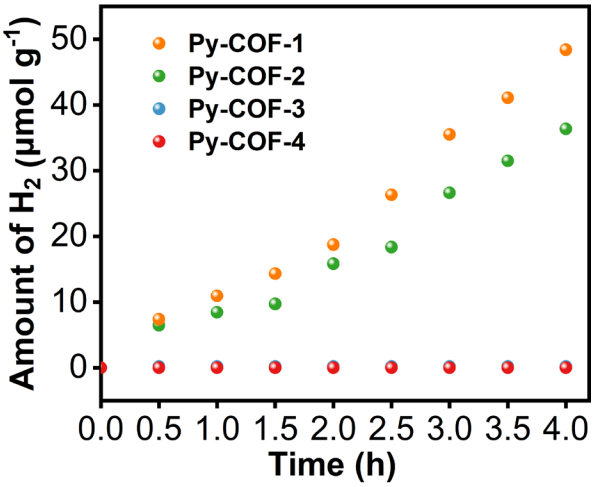

Figure S23. Photocatalytic H_2 evolution performances of Py-COFs with triethanolamine as the sacrificial agent.

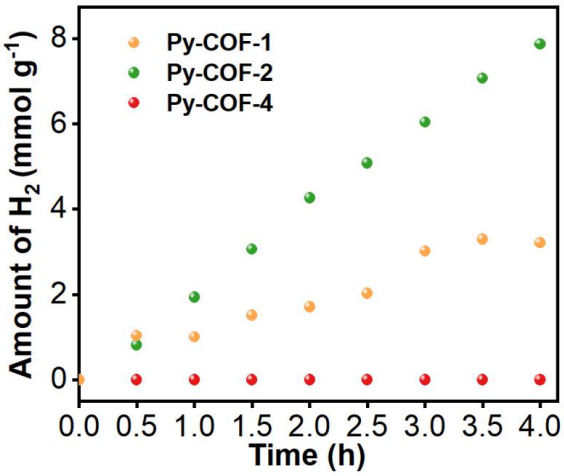

Figure S24. Photocatalytic H_2 evolution performances of Py-COF-1, Py-COF-2, and Py-COF-4 with ascorbic acid as the sacrificial agent.

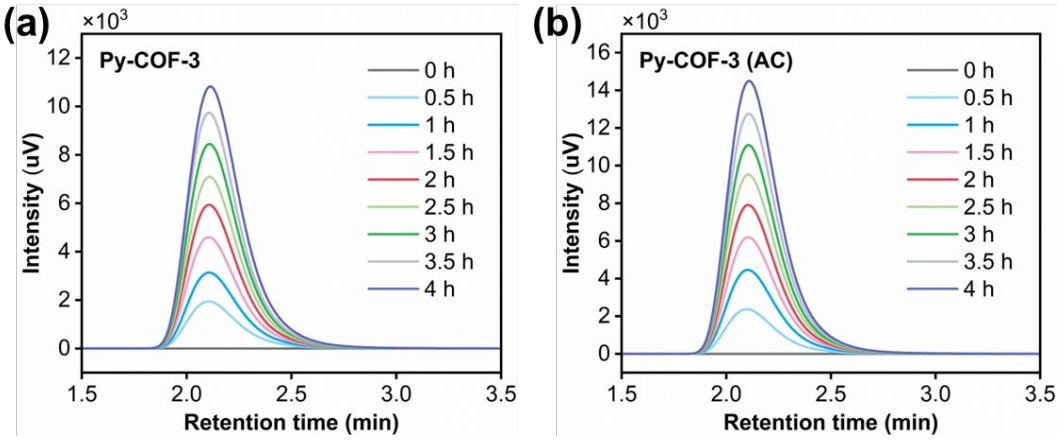

Figure S25. The GC curves for H_2 gas production in Py-COF-3 and Py-COF-3 (AC).

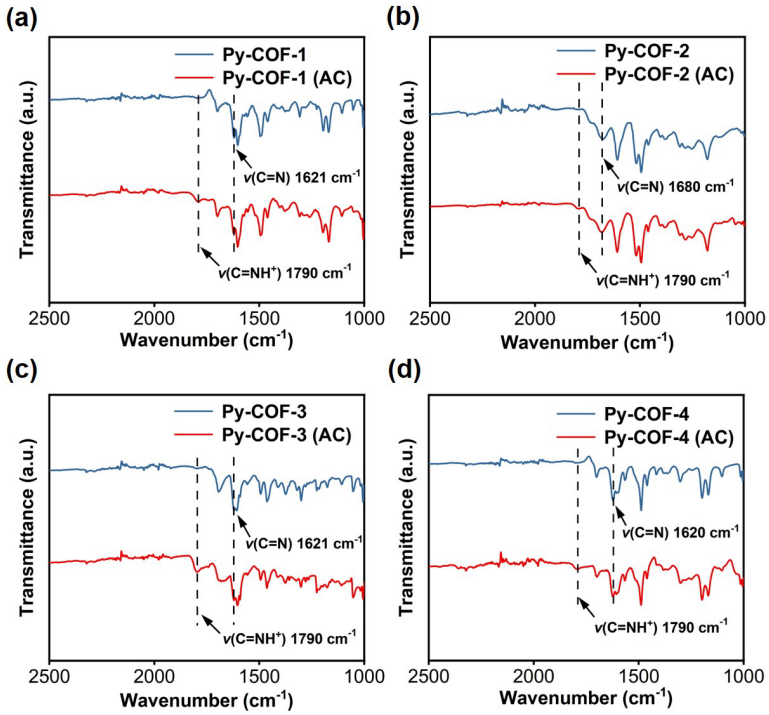

Figure S26. FT-IR spectra of (a) Py-COF-1 (AC), (b) Py-COF-2 (AC), (c) Py-COF-3 (AC) and (d) Py-COF-4 (AC).

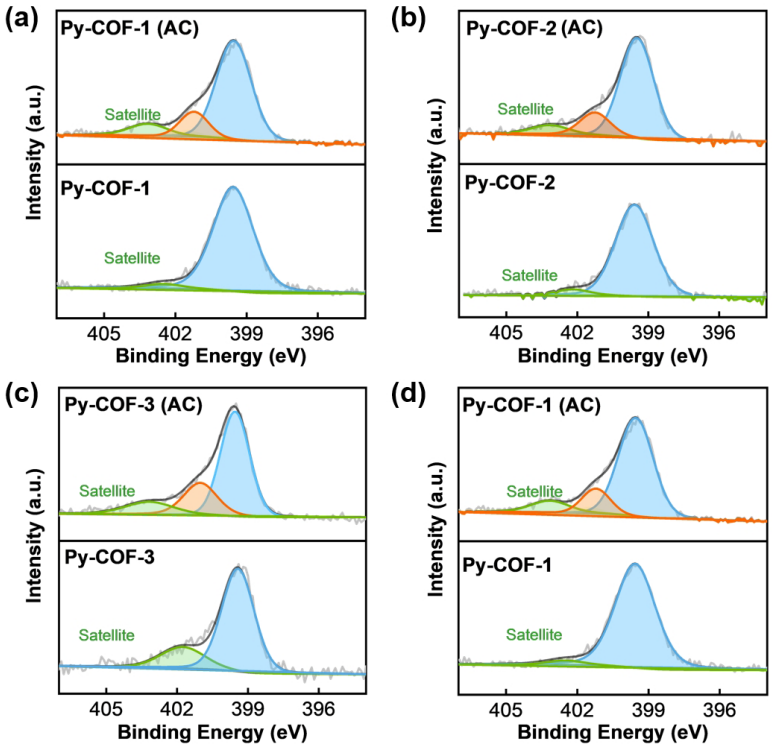

Figure S27. The N 1s XPS spectra of the Py-COFs before and after protonation. Blue, orange, and green regions represented the imine type N, protonated type N, and satellite N, respectively.

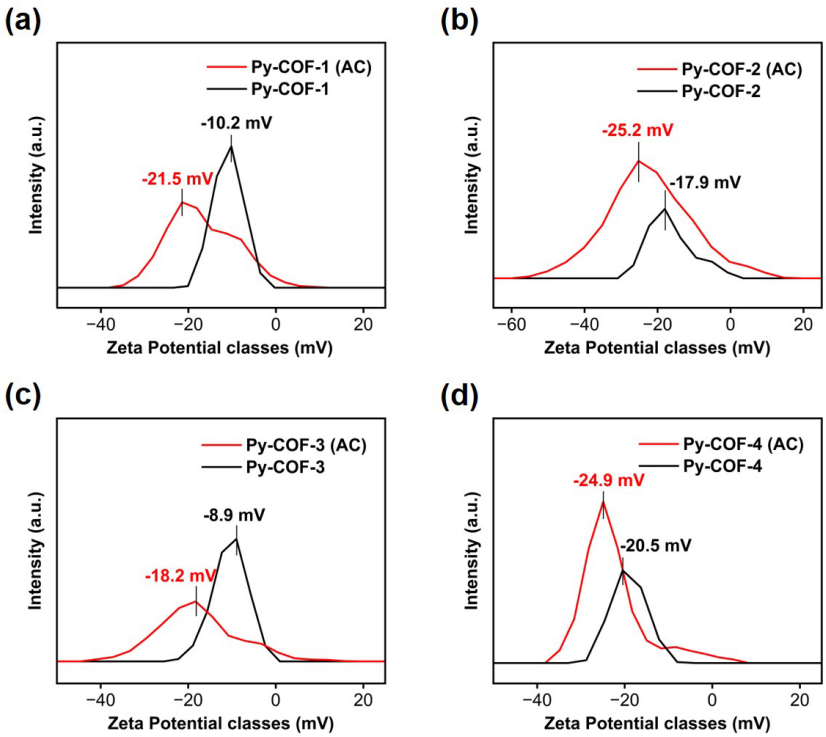

Figure S28. The zeta potentials of Py-COFs before and after protonation.

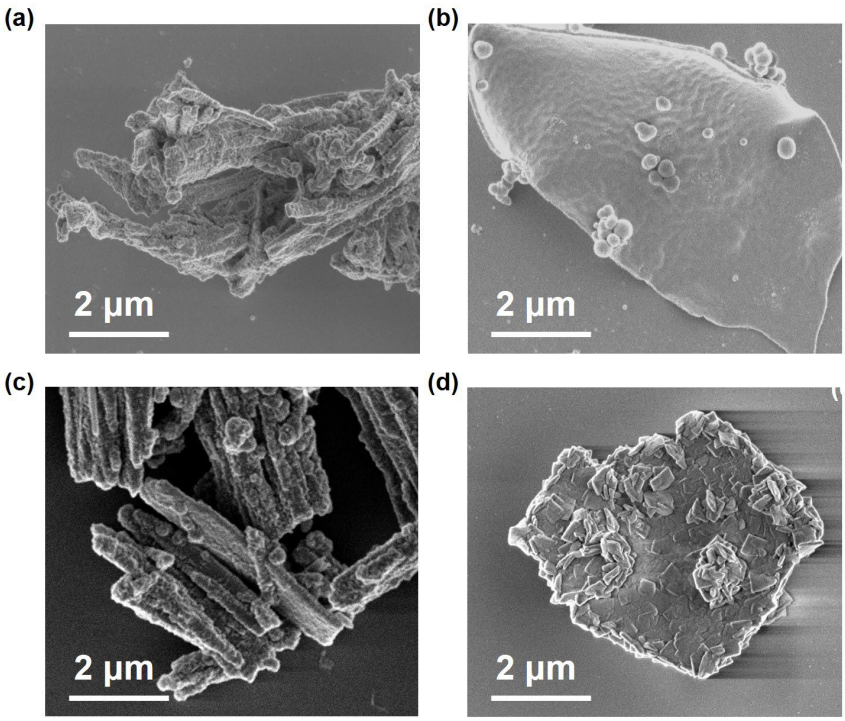

Figure S29. SEM images of (a) Py-COF-1 (AC), (b) Py-COF-2 (AC), (c) Py-COF-3 (AC) and (d) Py-COF-4 (AC).

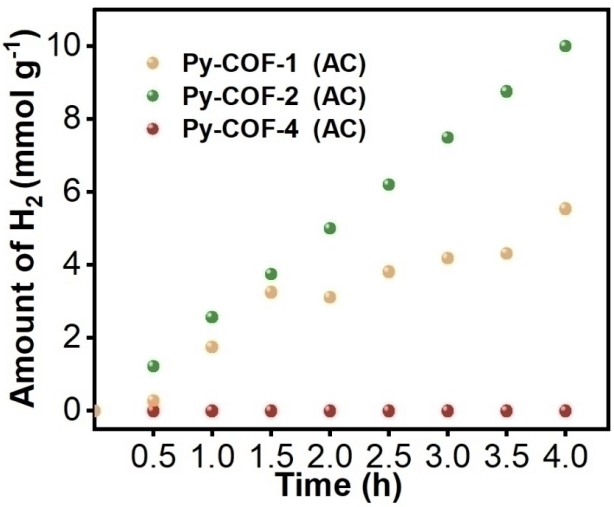

Figure S30. The photocatalytic H_2 production of Py-COF-1 (AC), Py-COF-2 (AC), and Py-COF-4 (AC).

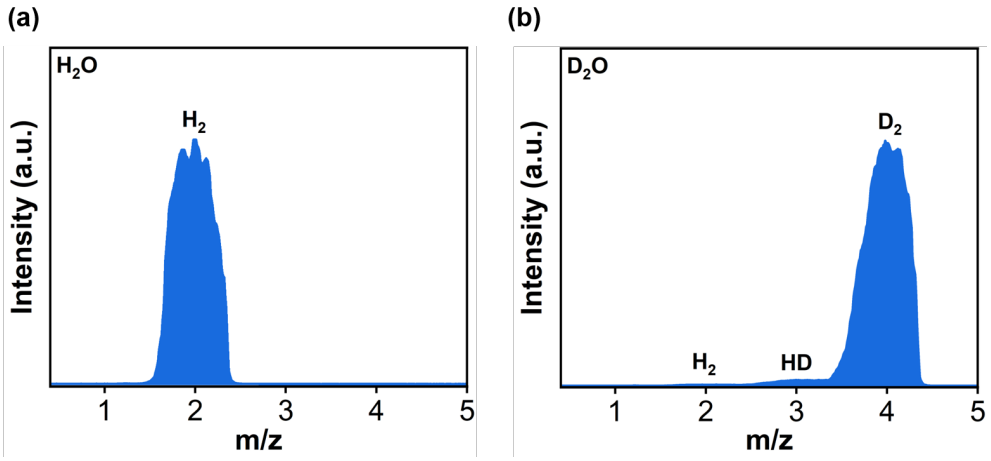

Figure S31. Hydrogen isotope labeling result of Py-COF-3 (AC) (10 mg catalyst in 15 mL H_2O (a) or D_2O (b), 10 μL H_2PtCl_6 (1 wt%, $\lambda >$ 420 nm, irradiated for 4 hours).

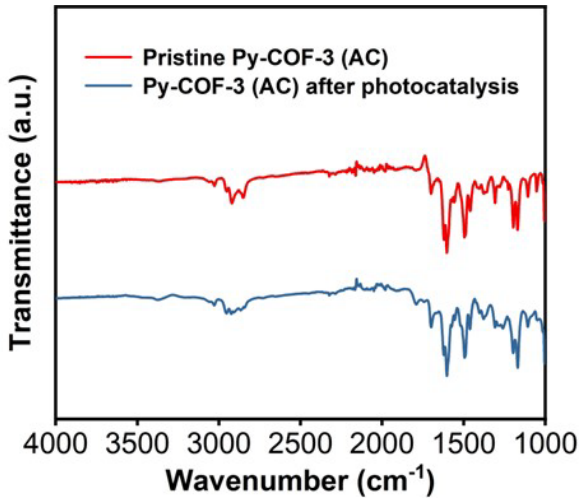

Figure S32. FT-IR spectra of Py-COF-3 (AC) before and after photocatalysis.

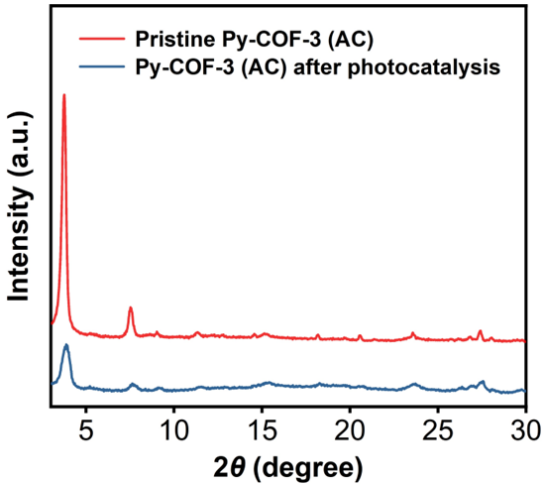

Figure S33. PXRD patterns of Py-COF-3 (AC) before and after photocatalysis.

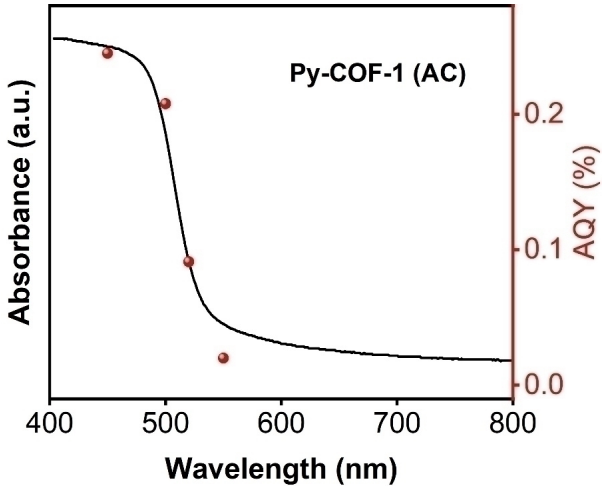

Figure S34. The AQYs of Py-COF-1 (AC).

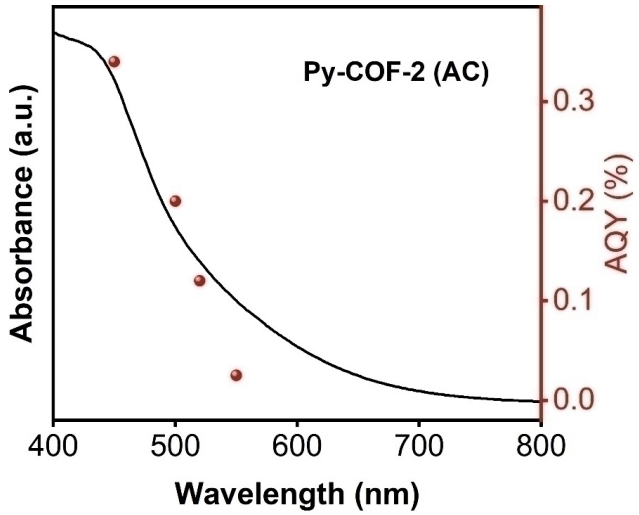

Figure S35. The AQYs of Py-COF-2 (AC).

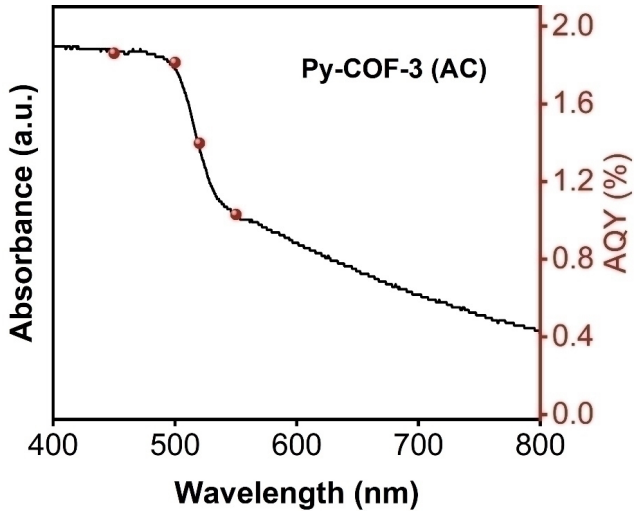

Figure S36. The AQYs of Py-COF-3 (AC).

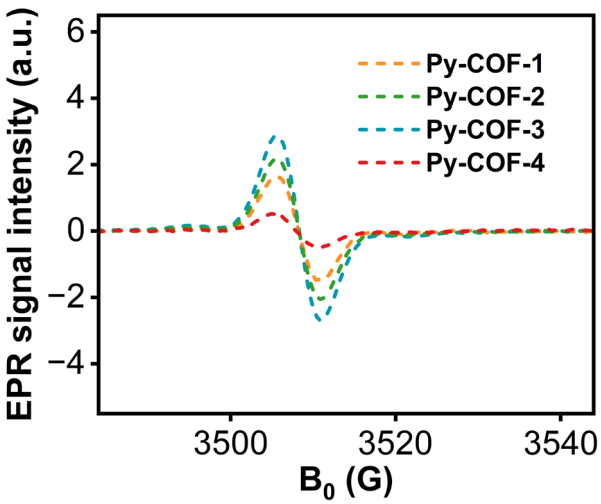

Figure S37. EPR spectra of Py-COF-1, Py-COF-2, Py-COF-3 and Py-COF-4 under

dark.

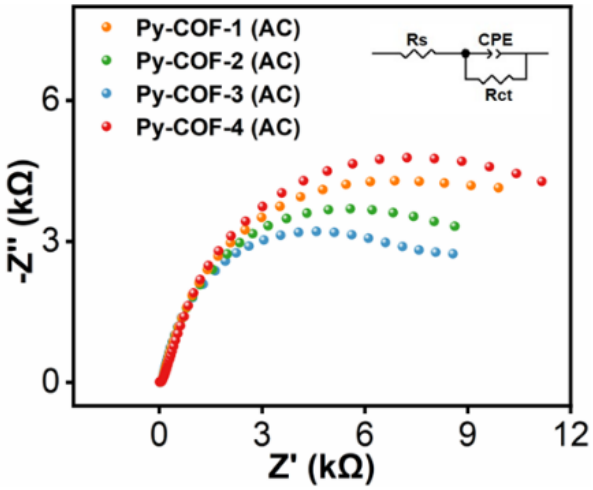

Figure S38. The Nyquist plots of the Py-COFs after protonation.

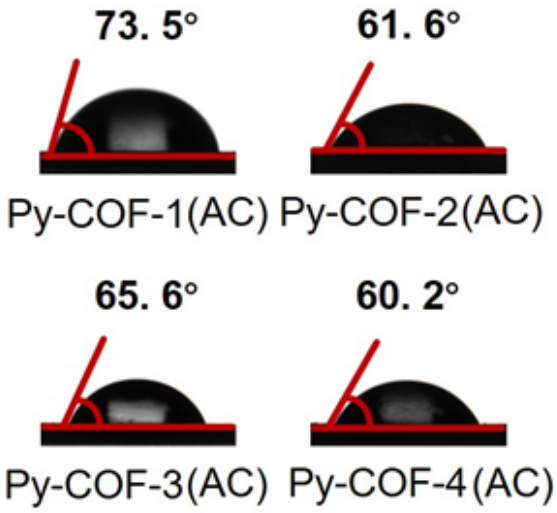

Figure S39. Water contact angle photos of the Py-COFs after protonation.

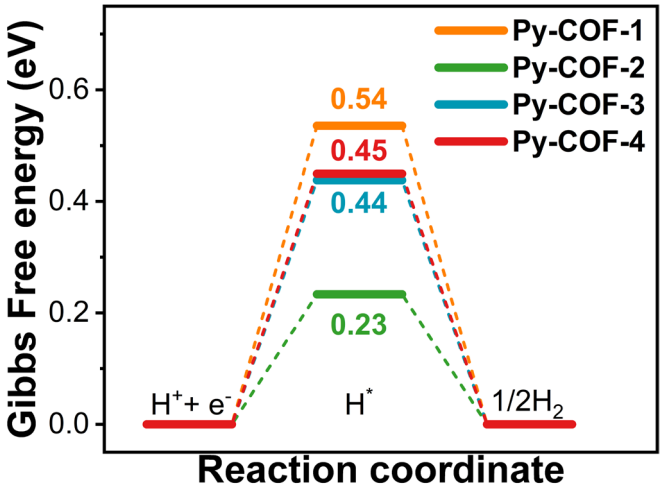

Figure S40. The Gibbs free energy diagram of hydrogen evolution reaction on imine N sites of Py-COFs.

Table S1. The deconvolution of the N 1s XPS spectra of Py-COFs.

Sample	Types of N	Position (eV)	Area	Ratio (%)	FWHM (eV)
Py-COF-1	imine N	399.5	5801		2.00
	satellite N	402.3	271		1.96
Py-COF-1 (AC)	imine N	399.5	4875		1.72
	protonated N	401.2	963	14.7%	1.38
	satellite N	403.2	693		1.90
Py-COF-2	imine N	399.5	3996		1.91
	satellite N	402.3	281		1.75
Py-COF-2 (AC)	imine N	399.5	4028		1.66
	protonated N	401.2	865	16.2%	1.50
	satellite N	403.2	459		1.89
Py-COF-3	imine N	399.5	2564		1.62
	satellite N	402.1	716		2.21
Py-COF-3 (AC)	imine N	398.5	4885		1.45
	protonated N	401.1	1883	24%	1.66
	satellite N	403.2	1074		2.41
Py-COF-4	imine N	399.5	2564		1.62
	satellite N	402.4	716		2.21
Py-COF-4 (AC)	imine N	399.5	3411		1.53
	protonated N	401.1	1292	25%	1.76
	satellite N	403.1	428		2.18

Table S2. The elemental analysis of Py-COFs before and after the protonation.

Sample	Molecular formula		C (%)	N (%)	H (%)
Py-COF-1	$C_{44}H_{26}N_4 \cdot 7H_2O$	Calcd.	71.72	7.60	5.47
		Found	72.01	6.95	4.76
Py-COF-2	$C_{44}H_{26}N_4 \cdot 5H_2O$	Calcd.	75.41	7.99	5.18
		Found	76.66	6.66	5.06
Py-COF-3	$C_{56}H_{34}N_4 \cdot 7H_2O$	Calcd.	75.66	6.30	5.44
		Found	75.11	5.50	4.00
Py-COF-4	$C_{56}H_{34}N_4 \cdot 2H_2O$	Calcd.	84.19	7.01	4.79
		Found	86.11	7.29	4.62
Py-COF-1 (AC)	$C_{44}H_{26}N_4 \cdot 9H_2O \cdot 0.8AC$	Calcd.	64.15	6.13	5.56
		Found	64.35	4.77	4.34
Py-COF-2 (AC)	$C_{44}H_{26}N_4 \cdot 5H_2O \cdot 0.8AC$	Calcd.	69.64	6.66	5.08
		Found	69.33	5.10	4.89
Py-COF-3 (AC)	$C_{56}H_{34}N_4 \cdot 7H_2O \cdot 1.8AC$	Calcd.	66.53	4.65	5.22
		Found	66.51	3.57	4.14
Py-COF-4 (AC)	$C_{56}H_{34}N_4 \cdot 2H_2O \cdot 1.8AC$	Calcd.	71.90	5.02	4.73
		Found	71.33	4.89	4.57

Table S3. The theoretical and actual amount of H_2 generation for Py-COFs.

Sample	Molecular formula	H^+ content (mmol/mg)	Theoretical H_2 production (mmol)	Actual H_2 production (mmol)
Py-COF-1 (AC)	$C_{44}H_{26}N_4 \cdot 0.588AC$	0.00083	0.0042	0.055
Py-COF-2 (AC)	$C_{44}H_{26}N_4 \cdot 0.648AC$	0.00090	0.0045	0.100
Py-COF-3 (AC)	$C_{56}H_{34}N_4 \cdot 0.960AC$	0.0010	0.005	0.782
Py-COF-4 (AC)	$C_{56}H_{34}N_4 \cdot 1.000AC$	0.0011	0.0055	0

Note: Theoretical H_2 production is calculated based on the protonated imine bonds as deduced from the XPS spectra; Actual H_2 production refers to the H_2 production of Py-COF-1 (AC) to Py-COF-4 (AC) for 4 hours.

Table S4. The simulated R_s and R_{ct} of the Py-COFs before and after protonation.

Sample	R_s (Ω)	R_{ct} (kΩ)	Sample	R_s (Ω)	R_{ct} (kΩ)
Py-COF-1	88.02	31.14	**Py-COF-1 (AC)**	53.43	11.37
Py-COF-2	84.23	26.46	**Py-COF-2 (AC)**	49.14	10.89
Py-COF-3	80.25	21.61	**Py-COF-3 (AC)**	47.77	7.93
Py-COF-4	90.72	38.66	**Py-COF-4 (AC)**	65.73	13.88

Table S5. Photocatalytic Hydrogen evolution performances of the reported Pyrene-based COFs photocatalysts.

Sample	Light	HER Activity (mmol g^{-1} h^{-1})	Sacrificial agent	Reference
2Br-COF	λ > 420 nm	13.61	ascorbic acid	4
TAPPy-DBTDP-COF	λ > 420 nm	12.7	ascorbic acid	5
TAPPy-BTDP-COF	λ > 420 nm	6.8	ascorbic acid	5
sp^2c-COFERDN	λ > 420 nm	2.12	ascorbic acid	6
Co/Zn-Salen-COF	λ > 420 nm	1.378	ascorbic acid	7
Py-HMPA	λ > 420 nm	37.925	ascorbic acid	8
Py-PDCA	λ > 420 nm	15.45	ascorbic acid	8
Py-MPA	λ > 420 nm	5.166	ascorbic acid	8
PY-DHBD-COF	λ > 420 nm	42.432	ascorbic acid	9
HIAM-0015	λ > 420 nm	17.99	ascorbic acid	10
HIAM-0016	λ > 420 nm	8.90	ascorbic acid	10
Py-N-DBT-COF	λ > 420 nm	0.82	ascorbic acid	11
Py-C-DBT-COF	λ > 420 nm	21.37	ascorbic acid	11
Py-ClTP-BT-COF	λ > 420 nm	8.875	ascorbic acid	12
Py-FTP-BT-COF	λ > 420 nm	2.875	ascorbic acid	12
Py-HTP-BT-COF	λ > 420 nm	1.078	ascorbic acid	12
PyTz-COF	AM 1.5	2.072	ascorbic acid	13
Benzd-COF	350 < λ < 780 nm	2.0273	triethanolamine	14
Azod-COF	350 < λ < 780 nm	0.5373	triethanolamine	14
Py-COF-1 (AC)	λ > 420 nm	1.3	ascorbic acid	***This work***
Py-COF-2 (AC)	λ > 420 nm	2.5	ascorbic acid	***This work***
Py-COF-3 (AC)	**λ > 420 nm**	**19.6**	**ascorbic acid**	***This work***

Section S4. Reference

1. G. Kresse, D. Joubert, *Phys. Rev. B*, 1999, **59**, 1758-1775.
2. G. Kresse, J. Furthmüller, *Comput. Mater. Sci.*, 1996, **6**, 15-50.
3. J.P. Perdew, K. Burke, M. Ernzerhof, *Phys. Rev. Lett.,* 1996, **77**, 3865-3868.
4. X. Deng, N. Gao and L. Bai, *Small*, 2024, **20**, 2311927.
5. N. Liu, S. Xie, Y. Huang, J. Lu, H. Shi, S. Xu, G. Zhang and X. Chen, *Adv. Energy Mater.*, 2024, **14**, 2402395.
6. E. Jin, Z. Lan, Q. Jiang, K. Geng, G. Li, X. Wang and D. Jiang, *Chem*, 2019, **5**, 1632-1647.
7. W. Zhou, Q.-W. Deng, H.-J. He, L. Yang, T.-Y. Liu, X. Wang, D.-Y. Zheng, Z.-B. Dai, L. Sun, C. Liu, H. Wu, Z. Li and W.-Q. Deng, *Angew. Chem. Int. Ed.*, 2023, **62**, e202214143.
8. Y. Liu, W.-K. Han, W. Chi, J.-X. Fu, Y. Mao, X. Yan, J.-X. Shao, Y. Jiang and Z.-G. Gu, *Appl. Catal. B: Environ.*, 2023, **338**, 123074.
9. Y. Li, L. Yang, H. He, L. Sun, H. Wang, X. Fang, Y. Zhao, D. Zheng, Y. Qi, Z. Li and W. Deng, *Nat. Commun.*, 2022, **13**, 1355.
10. C.-Q. Han, J.-X. Guo, S. Sun, Z.-Y. Wang, L. Wang and X.-Y. Liu, *Small*, 2024, **20**, 2405887.
11. X. Ren, J. Sun, Y. Li and F. Bai, *Nano Res.*, 2024, **17**, 4994-5001.
12. W. Chen, L. Wang, D. Mo, F. He, Z. Wen, X. Wu, H. Xu and L. Chen, *Angew. Chem. Int. Ed.*, 2020, **59**, 16902-16909.
13. W. Li, X. Huang, T. Zeng, Y. A. Liu, W. Hu, H. Yang, Y.-B. Zhang and K. Wen, *Angew. Chem. Int. Ed.*, 2021, **60**, 1869-1874.
14. H. Wu, X. He, X. Du, D. Wang, W. Li, H. Chen, W. Fang and L. Zhao, *Small*, 2023, **19**, 2304367.